Immobilized Enzyme Reactors. Diffusion/Convection, Kinetics, and a Comparison of Packed-Column and Rotating Bioreactors for Use in Continuous-Flow Systems

Pablo Richter,[†] Beatriz López Ruiz,[‡] Mercedes Sánchez-Cabezudo,[‡] and Horacio A. Mottola*

Department of Chemistry, Oklahoma State University, Stillwater, Oklahoma 74078-3071

The roles of chemical kinetics and mass transfer in two types of bioreactors (packed-column reactors and rotating disk bioreactors), used with continuous-flow sample/reagent(s) processing, are discussed in detail. A normalized quantitative comparison between these types of reactors clearly shows that rotating disk reactors afford a significantly more efficient utilization of immobilized active sites and permit the effective utilization of very small amounts of biocatalysts. Glucose oxidation by dissolved oxygen, catalyzed by immobilized glucose oxidase (EC 1.1.3.4), was used as a chemical model. The H_2O_2 product of the enzyme-catalyzed reaction was detected at a platinum working electrode for quantitation of the data.

The design and performance of reactors utilizing immobilized enzymes as analytical reagents for use with continuous-flow sample/reagent(s) processing attract considerable contemporary interest among analytical chemists. The use of immobilized enzymes in clinical, food, and environmental analyses justifies such interest as well as the publication of specialized monographs.[1] Most enzymes, however, are relatively expensive reagents, even when the added shelf stability afforded by many immobilization chemistries is taken into consideration. Consequently, in the design of bioreactors for chemical analysis, configurations that afford the maximum utilization of the immobilized active sites are a desirable goal.

For both segmented and unsegmented continuous-flow systems, packed-column reactors are by far the most common. These reactors, however, preclude the full utilization of all immobilized active sites. Despite relatively long residence times in the reactor (low flow rates), the geometric configuration of the packing and diffusional constraints do not permit full utilization. The popularity of packed-column bioreactors stems from the ease of preparation and insertion in continuous-flow manifolds; however, alternatives (e.g., rotating reactors[2]) involve relatively little added complication and, as demonstrated in this article, afford a considerably fuller utilization of immobilized active sites. Mass transport (diffusion/convection) and chemical kinetics are the physicochemical factors that dictate the degree of utilization of immobilized active sites, and a discussion of them is included to introduce the comparison between packed-column and rotating reactors presented here.

EXPERIMENTAL SECTION

Apparatus. Microcolums were made of Tygon tubing (2.0 cm long, 2.0 mm i.d.). The bioreactor/amperometric detection unit used was of the type described earlier, with the stationary platinum ring electrode located just above the rotating reactor.[3] The original design was modified by attaching a small cylinder of Teflon (3.5 mm diameter × 4 mm length) terminated in conical form, which was inserted in a well of similar dimensions and form. The well was machined in the center of the indentation in the lower cell body for location of the rotating reactor. This assured stability upon rotation at high rpm values. Change in cell volume was accomplished by rotation of a spacer ring that changed the relative position of the upper cell body with respect to the lower cell body with the unit assembled. The volume of the cell was 75 μL, and the gap between the rotating disk and the electrode was 0.75 mm in the comparison studies, or varied as indicated.

The overall basic setup and the continuous-flow/stopped-flow/continuous-flow operation have been described previously.[2] The applied potential at the platinum working electrode, for H_2O_2 detection, was +0.600 V vs a Ag/AgCl, 3.0 M NaCl reference. Spectrophotometric measurements, for activity determination, were performed with a Perkin-Elmer Lambda 3840 linear diode array spectrophotometer operated by a Perkin-Elmer 7300 computer and using 1-cm glass cells. All pH measurements were made with a Model 701A Orion digital pH meter equipped with an epoxy-body combination electrode (Sensorex, Westminster, CA).

Reagents and Solutions. All reagents used were of analytical reagent grade except as noted. Aminopropyl controlled-pore glass (average pore size 700 Å, 80−120 mesh, amine content 100 μmol g^{-1}) was from Sigma (St. Louis, MO), as was glucose oxidase (EC 1.1.3.4) from *Aspergillus niger*, Type VII (23 600 units g^{-1}). Glucose oxidase catalysis of the oxidation of glucose by dissolved oxygen was adopted as chemical model here because of the relative low cost of the enzyme and convenience of H_2O_2 monitoring. Glutaraldehyde (25% w/w aqueous solution) was from Aldrich Chemical Co. (Milwaukee, WI). The solution used as carrier was phosphate buffer of pH 7.00 and 0.10 M total phosphate concentration.

Enzyme Immobilization. Glucose oxidase was immobilized via the glutaraldehyde attachment to the aminopropyl-modified

[†] Present address: Departamento de Química, Facultad de Ciencias, Universidad de Chile, P.O. Box 653, Santiago, Chile.

[‡] Present address: Sección Departamental de Química Analítica, Facultad de Farmacia, Universidad Complutense, 28040 Madrid, Spain.

(1) Valcárcel, M.; Luque de Castro, M. D. *Flow-Through (Bio)Chemical Sensors*; Elsevier: Amsterdam, 1994.

(2) Matsumoto, K.; Baeza Baeza, J. J.; Mottola, H. A. *Anal. Chem.* **1993**, *65*, 636−639.

(3) Baeza Baeza, J. J.; Matsumoto, K.; Mottola, H. A. *Anal. Chim. Acta* **1993**, *283*, 785−793.

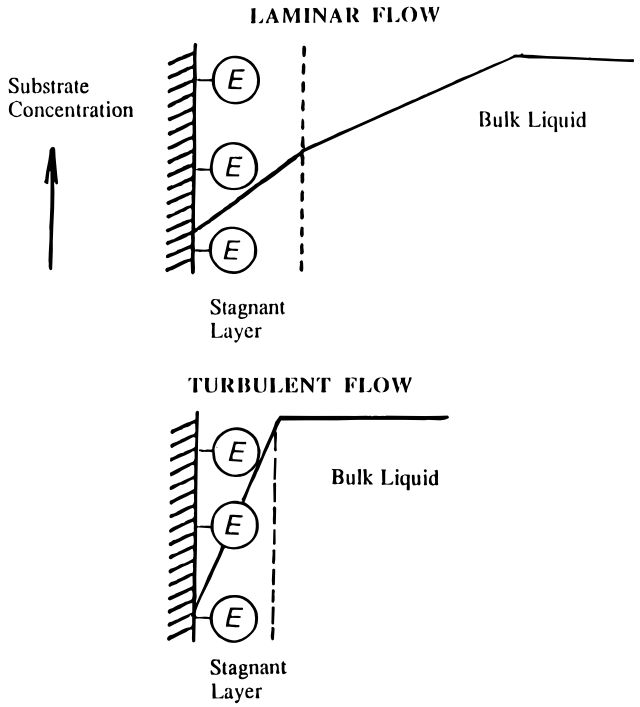

Figure 1. Idealized illustration of the substrate concentration gradients at the surface of an immobilized enzyme system under laminar and turbulent flow conditions. The illustration anticipates that diffusion can be rate limiting under laminar instead of turbulent flow. *E* represents the immobilized enzyme preparation.

controlled-pore glass.[2] A single stock preparation was used throughout the overall work comparing packed columns and rotating disks. Enzyme activity of this preparation was checked daily by using the *o*-dianisidine photometric procedure on 2-mg portions (Catalog No. 510-DA, Sigma, St. Louis, MO). Activity values were calculated from initial rate slopes and expressed per unit weight of enzyme preparation (i.e., in units of $\Delta A\ s^{-1}\ mg^{-1}$).

Preparation of Reactors. Immediately after measurement of the normalized activity, a portion of the enzyme preparation was fixed on the rotating reactor with double-coated sticking tape as already described,[2] and another portion was used as a slurry to pack well the column reactor. The weight of immobilized-enzyme preparation contained in each reactor was accurately determined by weighing, with an uncertainty of ±0.05 mg.

Calculation of Responses. Two types of measurements were utilized: initial rate measurements and estimation of the area under the recorded transient peaks by integration.[3] Values so obtained were then normalized per unit weight and unit activity of the given preparations as needed.

RESULTS AND DISCUSSION

Mass Transfer Using Immobilized Catalytic Centers. The concentration profiles in the vicinity of an immobilized enzyme preparation are illustrated in Figure 1. Arrival of substrate molecules to the active site of the immobilized biocatalyst is dictated by molecular diffusion within the diffusion (stagnant) layer, ∂, and this is a function of the mass transfer coefficient, $m = D/\partial$ (D is the molecular diffusion coefficient), and the concentration gradient,

$$d[S_s]/dt = m([S_b] - [S_s]) \qquad (1)$$

where S_s is the substrate at the surface of the immobilized enzyme preparation (vicinity of enzyme active site) and S_b is the substrate in the bulk of the solution. A decrease in the thickness of the diffusion layer, ∂, and an increase in concentration gradient, $[S_b] - [S_s]$, will result in an increase in the rate of substrate arrival at the site where the immobilized enzyme resides.

Experimental conditions in unsegmented continuous-flow systems result in predominantly laminar flow within the sample plug containing the analyte.[4] In laminar flow, each layer of solution flows in parallel paths; solutes diffuse through each layer and the diffusion layer to reach the active site, while in turbulent flow solutes diffuse directly from the bulk solution through the diffusion layer. As such, the concentration gradient developed within the diffusion layer boundaries is larger under turbulent than laminar flow conditions. Turbulent flow, however, would remove the advantages of reasonable residence times within the packed column afforded by laminar flow. It would also increase back-pressure problems if a small-particle-size packing material is used to increase the nominal activity of the immobilized enzyme and compensate for a short residence time. In other words, turbulent flow complicates matters under continuous-flow operation.

Since the inert supports used to anchor the biocatalyst are not ideally smooth, formation of local turbulence is realized at any irregularities or pronounced curvatures. Local turbulence at cylindrical/spherical bodies, protruding surface irregularities, sharp bends, or surface depressions in packed columns develop at Reynolds numbers, *Re*, between 1 and 100.[5] Hamilton et al.[6] have quoted *Re* values in the range 0.003−0.2 (velocity up to 0.18 cm s^{-1}), and values of $Re \approx 20$ are needed for turbulence around protruding surface irregularities.[7] Average velocities in typical flow injection systems are 3−4 times as high; hence, one would suspect that, when using packed columns of 1−2 mm i.d. and flow rates of about 1.0 mL min^{-1}, local *Re* numbers should be barely below 1 or 1 at most. Therefore, local turbulence would rarely be encountered with packed columns and unsegmented continuous-flow processing. Local turbulence, if present, would not help in improving the diffusional constraints of mass transfer when using the typical packed-column reactors, and strategies incorporating convectional mass transfer should provide a competitive alternative. The discussion presented here is focused on substrate arrival at the active site; similar considerations should also apply to transport of the product of the enzyme-catalyzed reaction from active site to the bulk of the solution.

Kinetics for Immobilized Catalytic Centers. Equation 1 mathematically describes the arrival of substrate at the active site. The conversion of substrate to products, with the participation of the enzyme active site, is equally important. If Michaelis−Menten behavior is assumed, the initial rate of disappearance of substrate at the surface of the immobilized enzyme preparation should be given by

$$-d[S_s]/dt = \{(IR)_{max}[S_s]\}/(K_M' + [S_s]) \qquad (2)$$

where $(IR)_{max}$ is the maximum initial rate representing the

(4) (a) Valcárcel, M.; Luque de Castro, M. D. *Flow Injection Analysis. Principles and Applications*; Ellis Horwood: Chichester, UK, 1987; p 59. (b) Ruzicka, J.; Hansen, E. H. *Flow Injection Analysis*, 2nd. ed.; Wiley: New York, 1988; p 98.

(5) Giddings, J. C. *Dynamics of Chromatography, Part I: Principles and Theory*, Dekker: New York, 1975; pp 217−224.

(6) Hamilton, P. B.; Bogue, D. C.; Anderson, R. A. *Anal. Chem.* **1960**, 32, 1782−1792.

(7) Stulík, K.; Pacáková, V. *Electroanalytical Measurements in Flowing Liquids*; Ellis Horwood: Chichester, UK, 1987; p 44.

situation in which all active sites are occupied by substrate at every time t and substrate concentrations are larger than the minimum needed for its realization. Consequently, $(IR)_{max} = k_{cat.}[E_{total,\,s}]$, in which $k_{cat.}$ is the rate coefficient for the conversion of the enzyme−substrate complex to products, and the utilization of all available enzyme active sites is given by $[E_{total,\,s}] \approx [ES_s]$. The apparent Michaelis−Menten constant is represented by K_M'.

The fact that imposing rotation to a platform bearing the immobilized enzyme preparation on its surface, and one which is in contact with solution containing the substrate, reduces the value of K_M' is well documented.[2,8] Under mass transfer control of the overall process, we can expect that $K_M' \gg [S_s]$, and the rate of conversion to product will be given by

$$-d[S_s]/dt = (k_{cat.}[ES_s][S_s])/K_M' \qquad (3)$$

As rotation decreases the value of K_M', the catalytic efficiency, $k_{cat.}/K_M'$, increases, and analytical signals should increase correspondingly. At sufficiently high rotation speeds, it can be expected that $[S_s] \gg K_M'$, and chemical kinetics controls the overall process because $-d[S_s]/dt \approx k_{cat.}[ES_s]$. In such a case, the analytical signal should, for all practical purposes, remain constant with increasing rotation velocity. Figure 2 illustrates that, indeed, the expected behavior is observed when the rotation velocity of the bioreactor is increased. Figure 2 illustrates the trend only for a cell volume of 225 μL, but the same was observed with cell volumes of 75 and 150 μL. The trend indicates that, up to velocities of about 1500 rpm, a decrease in the thickness of the stagnant layer improves mass transfer to and from the immobilized enzyme active sites. Beyond 1500 rpm, the initial rate is constant, and chemical kinetics controls the overall process. As observed earlier,[2] slightly better linearity is obtained with plots based on the square root of the rotation velocity of the disk bearing the immobilized enzyme preparation. It is of interest to note that, although the mass transfer is being realized under conditions similar to a thin-layer bounded diffusion with imposed turbulence, the dependence seems to agree better with the response at a rotating disk electrode and the Levich's equation[9] (see Figure 2B). Levich's equation, however, is derived for conditions of semiinfinite diffusion (the walls of the "cell" can be considered to be at infinity), and fast laminar flow predominates at the rotating surface.

Effect of Cell Volume. Since the signal response is due to a product of the enzyme-catalyzed reaction, H_2O_2, in this case an increase in cell volume should linearly decrease the value of initial rate. Figure 3 shows plots of initial rate as a function of cell volume, which was varied by increasing the gap between the working electrode and the reactor. In an attempt to minimize the dilution effect, the sample size was changed accordingly to ensure that the entire volume of the cell was filled with the sample. Figure 3 illustrates the dependence on cell volume at rotation velocities lower and higher than that at which the process becomes independent of rotation velocity (i.e., when chemical kinetics is rate determining). The general trend is represented by two straight lines and is independent of rotation velocity, with

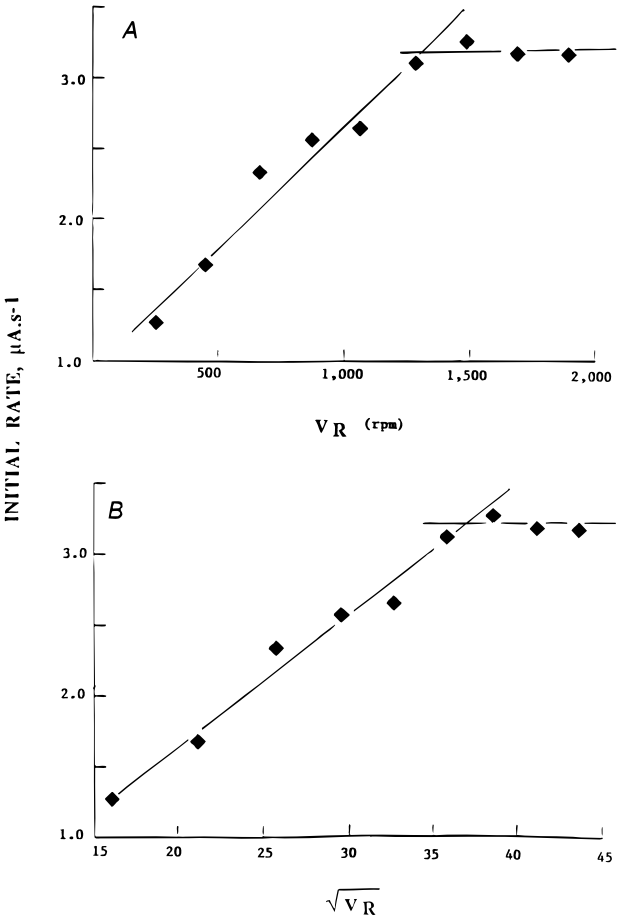

Figure 2. Effect of reactor rotation velocity on initial rates measured under stopped-flow conditions. Cell volume was 225 μL (gap between electrode and reactor, 2.25 mm). (A) Plot as a function of rotation velocity. (B) Plot as a function of the square root of the rotation velocity. Regression coefficients for the ascending straight line: (A) 0.976 and (B) 0.990. Glucose concentration, 0.50 mM, 0.10 M phosphate buffer of pH 7.00. Flow stopped for 60 s during measurement.

the intercept of both segments at about the same cell volume (~200 μL). Above this volume, the initial rate decreases with cell volume at a rate that is not significantly different at different rotation velocities, but below such a volume it increases dramatically with an increase in rotation velocity (roughly tripling from 258 to 1900 rpm). Apparently, two different mass transfer regimes from reactor to detector dominate below and above a cell volume in the vicinity of 200 μL. Below such a volume convection seems to predominate, and above it molecular diffusion starts to compete. Qualitatively, these trends seem to parallel, in part, the qualification of different "diffusion" coefficients at different distances from the rotating surface.[10]

Quantitative Comparison of Catalytic Efficiency between Rotating Bioreactors and Conventional Packed-Column Reactors. Using the glucose/glucose oxidase model system, the comparison was guided by utilizing normalized data and a single batch of enzyme preparation in all the work. The activity of the enzyme preparation was checked daily by using the *o*-dianisidine photometric method and before preparation and use of both types of reactors. The weight of controlled-pore-glass-immobilized

(8) (a) Kamin, R. A.; Wilson, G. *Anal. Chem.* **1980**, *52*, 1198−1205; (b) Shu, F. R.; Wilson, G. S. *Anal. Chem.* **1976**, *48*, 1679−1686. (c) Raba, J.; Mottola, H. A. *Anal. Chem.* **1994**, *66*, 1485−1489. (d) Raba, J.; Mottola, H. A. *Anal. Biochem.* **1994**, *220*, 297−302. (e) Raba J.; Li, S.; Mottola H. A. *Anal. Chim. Acta* **1995**, *300*, 299−305.

(9) Levich, V. G. *Physicochemical Hydrodynamics*; Prentice-Hall: Englewood Cliffs, NJ, 1962.

(10) Opekar, F.; Beran, P. *J. Electroanal. Chem. Interfacial Electrochem.* **1976**, *69*, 1−105.

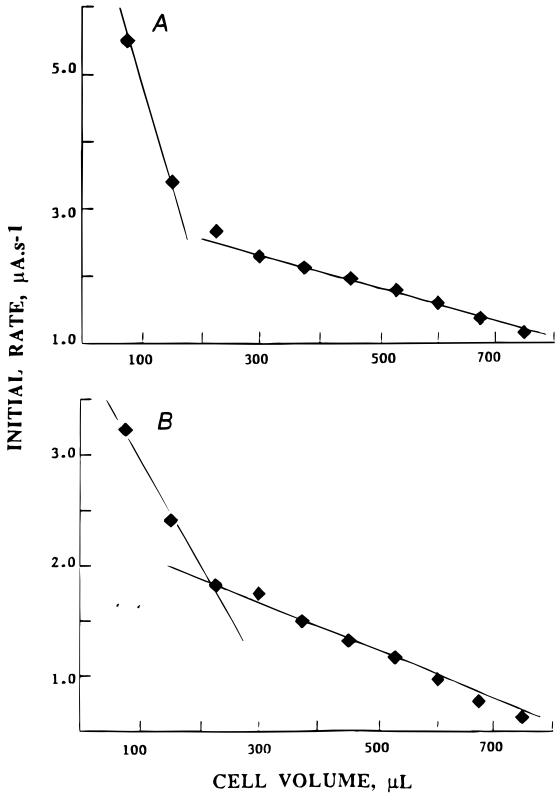

Figure 3. Effect of cell volume on initial rates measured under stopped-flow conditions. (A) Reactor rotation velocity, 1900 rpm. (B) reactor rotation velocity, 258 rpm. Glucose concentration, 0.50 mM, 0.10 M phosphate buffer of pH 7.00. Flow stopped for 60 s during measurement.

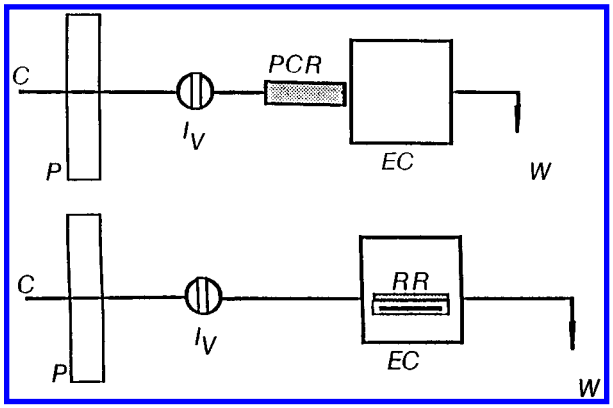

Figure 4. Block diagrams of the single line continuous-flow systems showing the location of the reactors compared in this work. The three-electrode detection arrangement was similar to the one described in ref 2. *C*, carrier line, 0.10 M phosphate buffer of pH 7.00; *P*, pump (Ismatec mv-ge, Model 7611-00, Cole-Parmer, Chicago, IL); I_V, sample injection valve (Rheodyne Type 50, Rheodyne, Cotati, CA); *PCR*, packed-column reactor; *EC*, electrochemical detection unit; *RR*, rotating reactor; *W*, waste.

Table 1. Comparative (Normalized) Enzymatic Efficiency of Rotating and Packed-Column Bioreactors[a]

	normalized signal, mC $(UA)^{-1}$		
		packed-column reactor	
normalized activity[b]	rotating reactor	flow rate 1.0 mL min^{-1}	flow rate 1.5 mL min^{-1}
8.5 ± 0.3	2.12 ± 0.05	0.156 ± 0.005	0.116 ± 0.003
8.5 ± 0.3	2.02 ± 0.05	0.130 ± 0.003	0.100 ± 0.002
8.4 ± 0.4	2.14 ± 0.07	0.129 ± 0.004	0.099± 0.002
8.4 ± 0.4	2.11 ± 0.02	0.127 ± 0.008	0.090 ± 0.003
8.4 ± 0.4	2.06 ± 0.05	0.134 ± 0.004	0.109 ± 0.003
mean	2.09 ± 0.05	0.135 ± 0.012	0.103 ± 0.010

[a] Uncertainties given as sample standard deviations of at least eight independent measurements. [b] 10^3 ΔA s^{-1} mg^{-1}.

enzyme preparation (CPG-E) was carefully recorded, and the normalized activity was calculated in ΔA s^{-1} mg^{-1}, where A is the absorbance at 460 nm. These values can be considered to be proportional to the number of enzyme active sites per unit weight of enzyme preparation in each of the two types of reactors compared. After each measurement of activity, the rotating disk reactor and packed column to be compared were prepared as described in the Experimental Section, and the respective amounts of CPG-E in each type of reactor were ascertained. The reactors were then incorporated into a single line continuous-flow manifold, like those illustrated in Figure 4. When using the packed-column reactor, the flow rate used was between 1.0 and 1.5 mL min^{-1}, values that are representative of the flow rates used in typical applications of packed reactor in flow injection analyses. Sample transport from injection to detection when using the rotating reactor was at a flow rate of 10 mL min^{-1}. The rotation velocity of the disk containing the enzyme preparation was 790 ± 20 rpm, determined as explained in ref 2. The injection volume in both cases was 85 μL, which completely filled the electrochemical cell used for detection.

After the electrochemical traces were recorded, the area under each transient signal was obtained by integration and normalized per unit activity in the corresponding reactor. The units of the normalized response are millicoulombs per unit activity [mC $(UA)^{-1}$]. The results of five comparative runs are summarized in Table 1. As can be seen from this table, the rotating bioreactor strategy increases by 15−20 times the enzymatic efficiency per active site. The rotation velocity used in this comparison (about 790 rpm) is about half of that needed for maximum utilization of the active sites (Figure 2), and as such the comparison has been made conservatively.

Sampling frequency has been and is an analytical figure of merit cited frequently as being significant when continuous-flow sample/reagent(s) processing is utilized. In using the packed-column reactor, the flow rate plays a critical role in dictating the sampling frequency. The time the flow is stopped and the flow rate play the same role when the rotating bioreactor is used. This is because of the signal integration approach used here and the fact that the return to baseline is flow dependent. Consequently, a perfectly normalized comparison is elusive, but some critical comparison is possible. Results for such comparison are summarized in Tables 2 and 3. Inspection of these tables indicates that a 5-s stopped-flow measurement with the rotating reactor provides sampling rate and enzymatic efficiency comparable to those of the packed column. In actuality, sampling rates close to those observed with the column can be obtained with up to 15 s stopped flow with a tripling of the biocatalytic efficiency. There is a trade-off, of course, for the rotating reactor between sampling rate and catalytic efficiency. Some sacrifice in the sampling rate must be accepted in order to take advantage of the efficient utilization of the fewer active sites immobilized on the surface of the rotating reactor. The authors of this paper believe that such

Table 2. Sampling Rate and Normalized Responses with Rotating Bioreactors as a Function of Flow Rate and Time the Flow Is Stopped for Acquisition of Rate Data[a]

	flow rate 1.0 mL min^{-1}		flow rate 1.5 mL min^{-1}	
stopped flow, s	sampling rate, samples h^{-1}	normalized signal, mC(UA)$^{-1}$	sampling rate, samples h^{-1}	normalized signal mC(UA)$^{-1}$
0	66.6 ± 1.7	0.090 ± 0.003	85.7 ± 1.6	0.060 ± 0.002
5	54.5 ± 1.5	0.160 ± 0.010	62.5 ± 1.7	0.100 ± 0.004
10	46.2 ± 1.5	0.250 ± 0.015	52.2 ± 1.4	0.200 ± 0.010
15	41.9 ± 1.3	0.380 ± 0.010	42.9 ± 1.4	0.310 ± 0.012
30	30.0 ± 1.3	0.764 ± 0.017	34.3 ± 1.5	0.755 ± 0.015
60	21.0 ± 0.5	2.06 ± 0.02	24.0 ± 0.7	1.93 ± 0.02
120	13.6 ± 0.5	5.45 ± 0.05	14.7 ± 0.5	4.69 ± 0.04
180	10.3 ± 0.4	8.83 ± 0.07	11.1 ± 0.5	7.21 ± 0.08

[a] Uncertainties are given as average deviation of average results obtained with three different (but similar) reactors.

Table 3. Sampling Rates Obtained with Packed Reactors as a Function of Flow Rate[a]

	flow rate 1.0 mL min^{-1}	flow rate 1.5 mL min^{-1}
sampling rate, samples h^{-1}	42.9 ± 1.4	50.0 ± 1.5
normalized signal, mC(UA)$^{-1}$	0.132 ± 0.003	0.108 ± 0.003

[a] Uncertainties are given as average deviation of average results obtained with three different (but similar) columns.

a sacrifice is unimportant when the effective use of very small amounts of relatively expensive biocatalysts is considered.

Comparison of Michaelis−Menten Constants and Maximum Initial Rates in Packed-Column and Rotating Bioreactors. The values of the apparent Michaelis−Menten constant, K_M', and maximum initial rate, $(IR)_{max}$, were evaluted for both types of reactors by using an adaptation of the Lineweaver−Burk plot.[2] Eight individually prepared rotating reactors and eight packed columns were included in this part of the study. Rotating reactors containing 2.3 ± 0.2 mg of CPG-E yielded average K_M' and $(IR)_{max}$ values of 1.2 ± 0.2 mM and (3.5 ± 0.2) × 10^2 nA s^{-1}, respectively, at a rotating velocity of 790 ± 20 rpm. Average values of K_M' and $(IR)_{max}$ for the eight columns (containing 2.5 ± 0.1 mg of CPG-E) were found to be 1.3 ± 0.3 mM and (3.0 ± 0.1) × 10^2 nA s^{-1}, respectively, with a flow rate of 1.0 mL min^{-1}. As was expected, K_M' values in packed reactors decreased when the length of the column was increased (representing a larger packing of immobilized active sites). The trend in decreasing values of K_M' in packed reactors levels off at about a value of 0.5 mM for packing 14 mg of CPG-E or more (Figure 5A). A similar trend has been observed during a study of the determination of Michaelis−Menten constants using a variable flow rate approach.[11] Figure 5 also shows, as a corollary of the studies reported here, that with a fixed amount of CPG-E, the same can be accomplished by increasing the rotation velocity of the rotating disk bearing the CPG-E.

Conclusions. The relative merits of rotating bioreactors in comparison to conventional column-packed reactors for use in conjunction with unsegmented flow sample/reagent(s) processing (e.g., minimal dispersion and maximal utilization of a very small number of immobilized active sites) are clear and are demonstrated in a quantitative manner in the work reported here. These

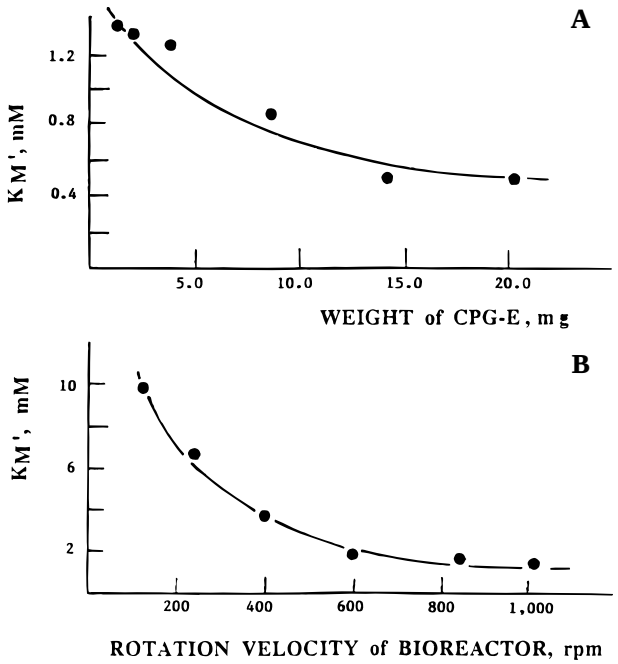

Figure 5. (A) Effect of increasing the length of the packed-column reactor (i.e., increasing the amount of CPG-E packed) on the value of K_M'. (B) Effect of disk bioreactor rotation velocity on the value of K_M'.

relative merits result from minimization of the limitations imposed by the rate of the enzyme-catalyzed reaction and the interplay of mass transfer in the form of diffusion and forced convection. This interplay and these limitations are introduced in this paper as background for a better understanding of the comparative results presented here.

ACKNOWLEDGMENT

P.R. acknowledges support from the American Chemical Society/Sociedad Chilena de Química program under National Science Foundation Grant No. INT-9412536. Support from the Comunidad de Madrid is acknowledged by B.L.R.

(11) Marcos, J.; Ríos, A.; Valcárcel, M. *Anal. Chim. Acta* **1993**, *283*, 429−438.

[⊗] Abstract published in *Advance ACS Abstracts,* April 1, 1996.